their frequencies saturate at about 30% and are lower than that of the base alloy. This means that the number of folds generated are few in the alloys with copper addition. Therefore, it is thought that the improvement of elongation for the 0.2%Cu and 0.5%Cu alloys is due to the decreases of frequency as compared with the base alloy, in addition to difficulties in development of folds with the progress of deformation. The reason that the elongation decreases in the 0.8%Cu alloy in spite of the same saturated frequency level of fold as the other alloys with copper, may relate to the same developed folds as the base alloy.

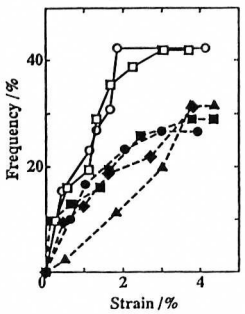

Fig.8 Frequencies of fold formation against the increase of elongation for the base alloy(○,□), the 0.2%Cu alloy(▲), the 0.5%Cu alloy(●,■) and the 0.8%Cu alloy(◆).

At the present investigation, it has not been understood yet that the reason why a displacement of grain boundary cannot be explained by F_{max} in the alloys with copper addition. Possibly, as the deformation within a grain differing from the base alloy by small amounts of copper addition seems more strongly to influence the localized deformation near grain boundaries than those of the base alloy, its influences on a displacement of grain boundary and a fold formation should be examined in detail.

4. CONCLUSION

The elongation in the alloys with small amounts of copper addition has been improved as compared with that in the base alloy. Localized deformation near grain boundary triple points were observed by STM in order to make clear the reason of the improvement of elongation. The results obtained are as follows:

(1) The fracture surfaces of the base alloy and the alloys with copper addition by tensile test have consisted in the mixture conditions of intergranular and transgranular fracture.

(2) From the STM observation, the characteristics of topographies of folds generated in these alloys have been similar to those of the alloy with excess silicon. The magnitude and the direction of F_{max} has seemed to provide the displacement of grain boundary in the base alloy, while in the alloys with copper addition, the direction of F_{max} has not been in agreement with that of a displacement observed at the grain boundary.

(3) The frequency of fold formation has increased with the progress of deformation and then saturated at about 40% in the base alloy, while those in the all alloys with copper addition have saturated at lower value of near 30% in spite of higher elongation than that of the base alloy.

REFFERENCES

[1]S.Ikeno, K.Matsuda, Y.Uetani and S.Tada : J. Jpn. Inst. Light Metals, **38**(1988), 394.

[2]Y.Uetani, H.Murase, K.Matsuda, H.Anada, S.Tada and S.Ikeno : J. Jpn. Inst. Metals, **58**(1994), 260.

[3]Y.Baba and A.Takashima : J. Jpn. Inst. Light Metals, **19**(1969), 90.

[4]K.Yokota, T.Komatsubara, T.Sato and A.Kamio : J. Jpn. Inst. Light Metals, **42**(1992), 149.

[5]Y.Uetani, T.Katayama, K.Matsuda, K.Terayama and S.Ikeno : J. Jpn. Inst. Light Metals, **47** (1997), 154.

[6]Y.Uetani, K.Ozaki, K.Matsuda, H.Anada, S.Tada and S.Ikeno : J. Jpn. Inst. Light Metals, **42** (1992), 400.

THE EFFECTS OF MAGNESIUM AND COPPER CONTENTS ON THE RESTORATION DURING HOT DEFORMATION OF Al-Mg-Cu ALLOYS

K. TAKIGUCHI, H. UCHIDA and H. YOSHIDA

Research & Development Center, Sumitomo Light Metal Industries, Ltd.
1-12, 3-chome, Chitose, Minato-ku, Nagoya 455-8670, JAPAN.

ABSTRACT In some studies about the deformation behavior of Al-Mg alloys during the hot deformation, it has been pointed out that the dynamic restoration occurs. To clarify the role of magnesium and copper on the restoration during the hot deformation is the purpose of this study. Al-Mg (3.0 to 8.0mass%) alloys with copper (0, 0.3mass%) were tensile tested at various temperatures from 350°C to 480°C and at an initial strain rate of $10^{-2}s^{-1}$. The subgrain formation from the original grain boundaries were observed. These dynamic restoration process enhanced the elongation of Al-Mg alloys at high temperature. The restoration occurred at the lower temperature and at the smaller strain with the magnesium contents. The cavity formation was enhanced by the precipitation of β-phase particles (Al_3Mg_2) during the hot deformation, and cavities increased with the magnesium contents. In the copper added alloys, T-phase particles (Al_6Mg_4Cu) precipitated during the hot deformation and prevented the formation of cavities at the grain boundaries, because these particles precipitated preferentially and inhibited the precipitation of β-phase particles along the grain boundaries.

Keywords : subgrain formation, dynamic restoration, precipitation, β-phase, T-phase.

1. INTRODUCTION

In recent years, Al-Mg alloys contain some copper had been used for automotive body sheets for the demand of weight saving. But these alloys have some problems during the hot deformation. It is well known that high solute magnesium atoms increase the frequency of cracking during the hot deformation, but on the other hand, these alloys exhibit the large elongation at the high temperature, if the condition of the hot deformation is appropriate.

In some studies about the deformation behavior of Al-Mg alloys during the hot deformation, it has been pointed out that the dynamic restoration[1] (dynamic recovery or dynamic recrystallization) occurs[2]-[5]. But, the relationships between dynamic restoration and precipitation of Al-Mg alloys have not been discussed[6]. The purpose of this study is to clarify the role of magnesium and copper on the restoration during the hot deformation.

2. EXPERIMENTAL PROCEDURE

Aluminum-magnesium (3.0 to 8.0mass%) alloys with copper (0, 0.3mass%) were used for this study. The chemical compositions of specimens are given in Table 1. The alloys were cast using direct chill technique into billets of 95mm diameter. The billets were homogenized for 8h at 470°C, and then, these were hot extruded at 400°C to the rod of 15mm diameter. The rod was drawn to

Table 1 Chemical compositions of specimens (mass%)

Alloy	Si	Fe	Cu	Mg	Ti
G33	0.04	0.03	0.26	3.01	0.02
G50	0.05	0.04	0.00	5.52	0.01
G53	0.04	0.04	0.27	5.45	0.01
G80	0.04	0.04	0.00	7.89	0.03
G83	0.05	0.04	0.31	8.00	0.03

12mm diameter, and then, the intermediate annealing was done for 5min at 520°C (G80 and G83 was annealed at 500°C) by salt bath. The rod was drawn to various reductions from 14.4% to 30.6% to control the average grain sizes of specimens about 100μm, and then the final annealing was done for 5min at 520°C (G80 and G83 was annealed at 500°C) by salt bath.

Cylindrical tensile specimen with 5mm diameter and with 15mm gage length were machined from the rod after final annealing. Tensile tests were performed at various temperatures from 350°C to 480°C, and then quenched immediately at some fixed strains to observe the microstructures after the hot deformation. The initial strain rate was controlled $10^{-2}s^{-1}$.

SEM-Electron Channeling Contrast (ECC) technique was used for large field observations of the grain structure with a JEOL JSM-6400 operated at 20kV. ECC samples were electrochemically etched in a solution of 94% ethanol and 6% perchloric acid at 0°C. Subgrain structures were observed by TEM bright field images with a JEOL JEM-200CX operating at 200kV, and the identification of precipitation was carried out by the analysis of selected area using diffraction patterns and the TEM dark field images. TEM samples were electrochemically etched in a solution of 75% methanol and 25% nitric acid at 20°C below zero. A X-ray diffractometer was also used to identify the precipitation with MAC Sci. M03X-HF. The X-ray incident angle was 1 degree.

3. RESULTS AND DISCUSSION

3. 1 The Effects of Magnesium Contents on the Restoration

The stress-strain curves of G33 (Al-3.0mass%Mg-0.3mass%Cu), G53 (Al-5.5mass%Mg-0.3mass%Cu), G83 (Al-8.0mass%Mg-0.3mass%Cu) alloys are illustrated in Fig. 1. Below 300°C, the curves showed the typical work hardening, and then, fracture occurred at low strain after local necking. At 350°C, the curves of G33 and G53 alloys showed the similar profiles at 300°C, but the curve of G83 alloy showed the peak at the initial stage of the hot deformation. At 380°C, the curves of G53 and G83 alloys showed the peak, and over 440°C, the curves of G33, G53 and G83 alloys showed the similar profiles. After the peak, flow stress showed the relatively constant stage and then decreasing slightly. The relatively constant stage of the curves occurred by the dynamic restoration process, and this phenomenon occurred at the lower temperature with the magnesium contents.

Figure 2 shows the SEM-ECC images of G33 and G83 alloys after the deformation at the true strain of 0.049, 0.095 and 0.262 at 440°C. As the true strain became larger, serrated grain boundaries were observed. It was considered that subgrain formed from the original grain boundaries, and then, these subgrains spread into the original grain. These dynamic restoration process enhanced the elongation of Al-Mg alloys at high temperature. The restoration (subgrain formation) occurred at the lower temperature and at the smaller strain with increasing the magnesium contents. The increase of magnesium contents had an effect of promoting the dynamic restoration .

Figure 3 shows the effect of true strain on cavity volume fraction. The cavity volume fraction increased with the true strain and with the magnesium contents. Figure 4 shows the TEM bright field image, TEM dark field image and diffraction pattern of β-phase (Al_3Mg_2) on the grain boundary in G80 alloy deformed at 380°C to failure. Figure 5 shows the qualitative analysis on β-phase particles measured by X-ray diffractometer in G50 alloy deformed at 380°C to failure and before testing. The β-phase particles are observed as a continuous film along the grain boundaries after the hot deformation. The cavity formation, which increased with the magnesium contents,

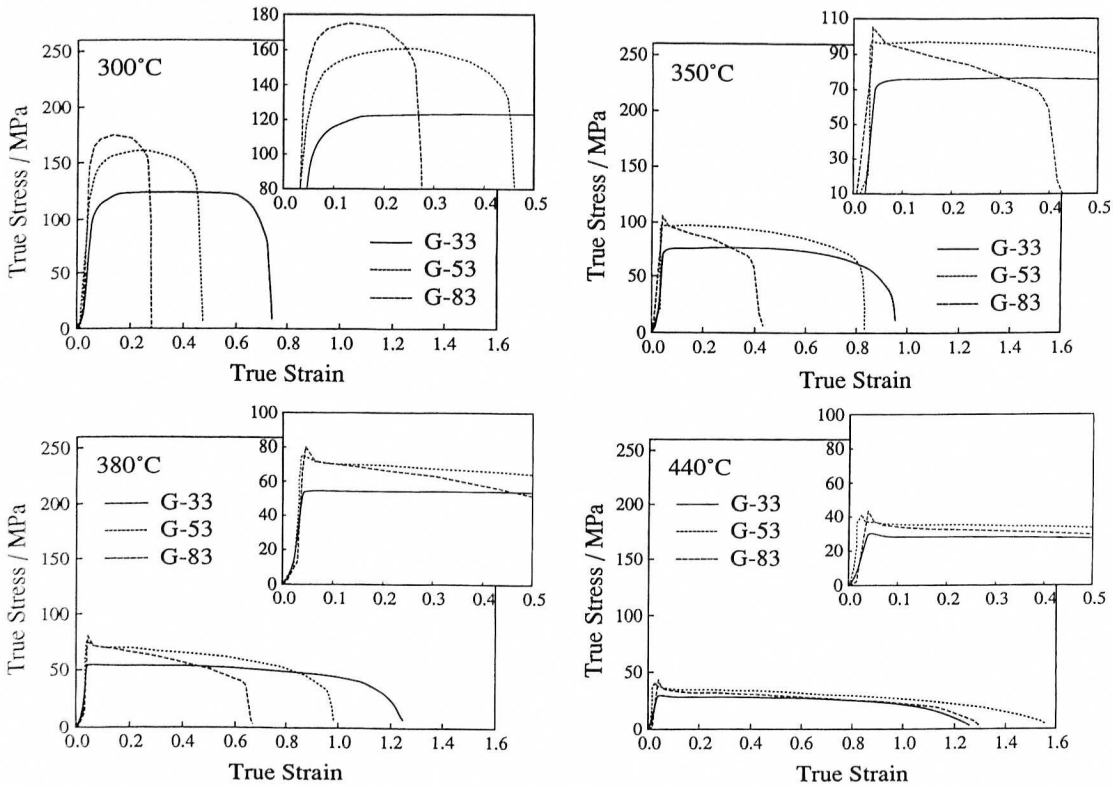

Fig. 1 Stress-strain curves of G33 (Al-3.0mass%Mg-0.3mass%Cu), G53 (Al-5.5mass%Mg-0.3 mass%Cu), G83 (Al-8.0mass%Mg-0.3mass%Cu) alloys

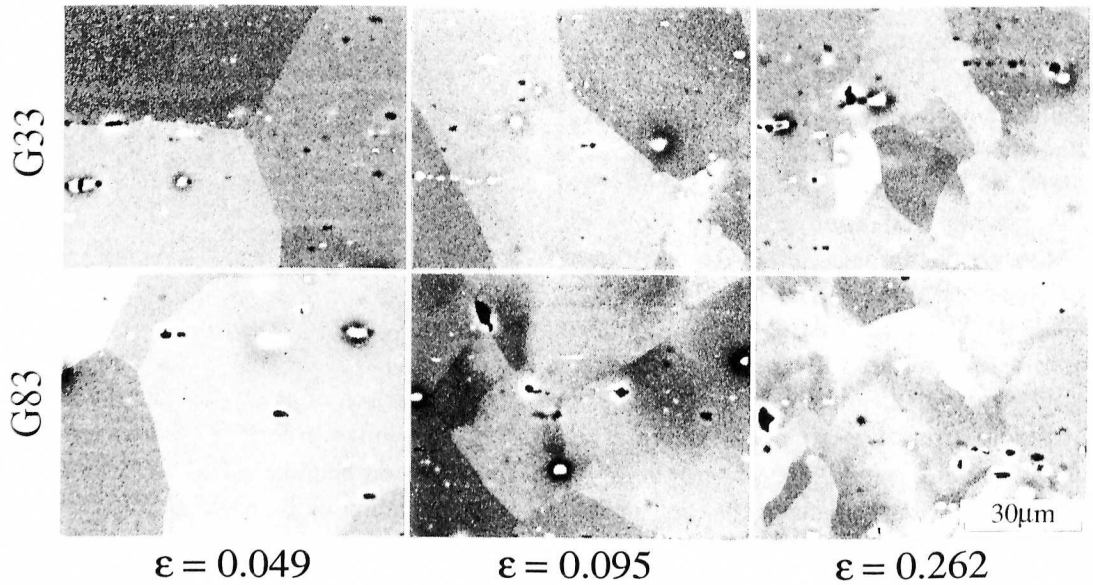

Fig. 2 SEM-ECC images of G33 (Al-3.0mass%Mg-0.3mass%Cu) and G83 (Al-8.0mass%Mg-0.3mass%Cu) alloys after the deformation at the true strain of 0.049, 0.095 and 0.262 at 440°C

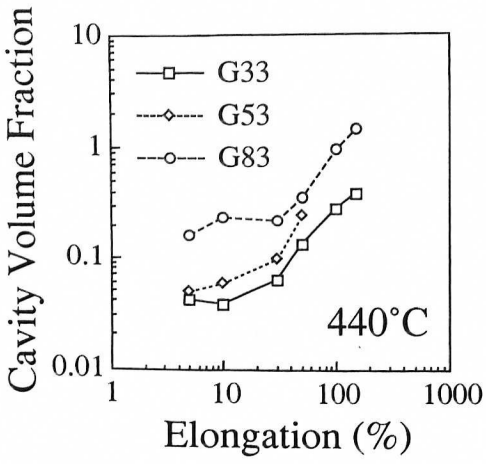

Fig. 3 Effect of nominal strain on cavity volume fraction

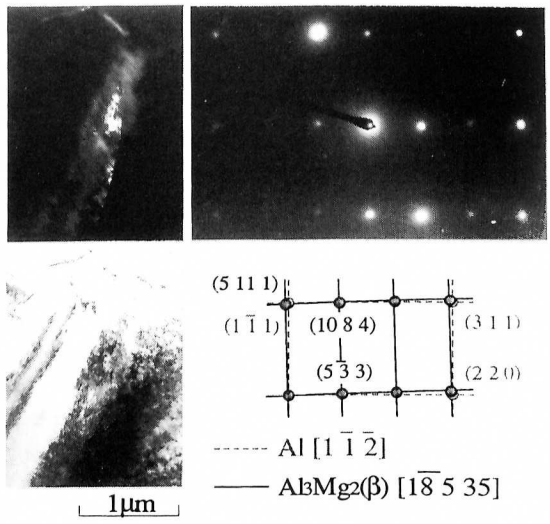

Fig. 4 TEM bright field image, TEM dark field image and diffraction pattern of β-phase on the grain boundary in G80 (Al-8.0 mass%Mg) alloy deformed at 380°C to failure

seemed to be enhanced by the precipitation of β-phase particles during the hot deformation.

The elongation of Al-Mg alloys at high temperature influenced by the dynamic restoration which increase the elongation, and the precipitation of β-phase particles along the grain boundaries which decrease the elongation.

3. 2 The Effects of Copper Addition on the Restoration

The stress-strain curves of G50 (Al-5.5mass%Mg) and G53 (Al-5.5mass%Mg-0.3mass%Cu) alloys are illustrated in Fig. 6. The addition of copper in Al-Mg alloys had an effect of increasing elongation. Figure 7 shows the TEM bright field image and diffraction pattern of T-phase (Al_6Mg_4Cu) in G53 alloy deformed at 380°C and a strain of 0.049. The T-phase particles precipitated discretely at the grain boundaries or in the grains. Fig. 8 shows the schematic comparison of cavity formation during the hot deformation. In the copper added alloy, T-phase particles precipitated during the hot deformation and prevented the formation of cavities at the grain boundaries, because the T-phase particles precipitated preferentially and inhibited the precipitation of β-phase particles (Al_3Mg_2) along the grain boundaries. The T-phase particles precipitated discretely and the β-phase particles precipitated along the grain boundaries, so the T-phase particles were less effective to form the cavities compared with the β-phase particles.

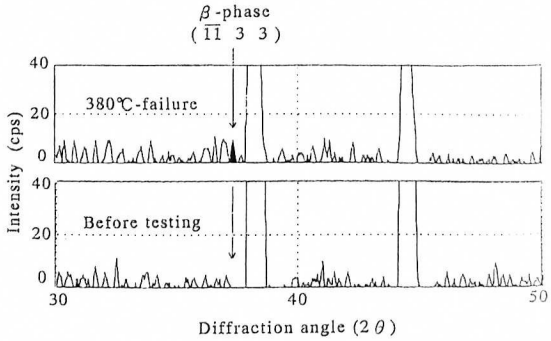

Fig. 5 Qualitative analysis on β-phase measured by X-ray diffractometer in G50 (Al-5.5 mass%Mg) alloy deformed at 380°C to failure and before testing

The large elongation at high temperature was obtained by controlling the contents of magnesium and copper.

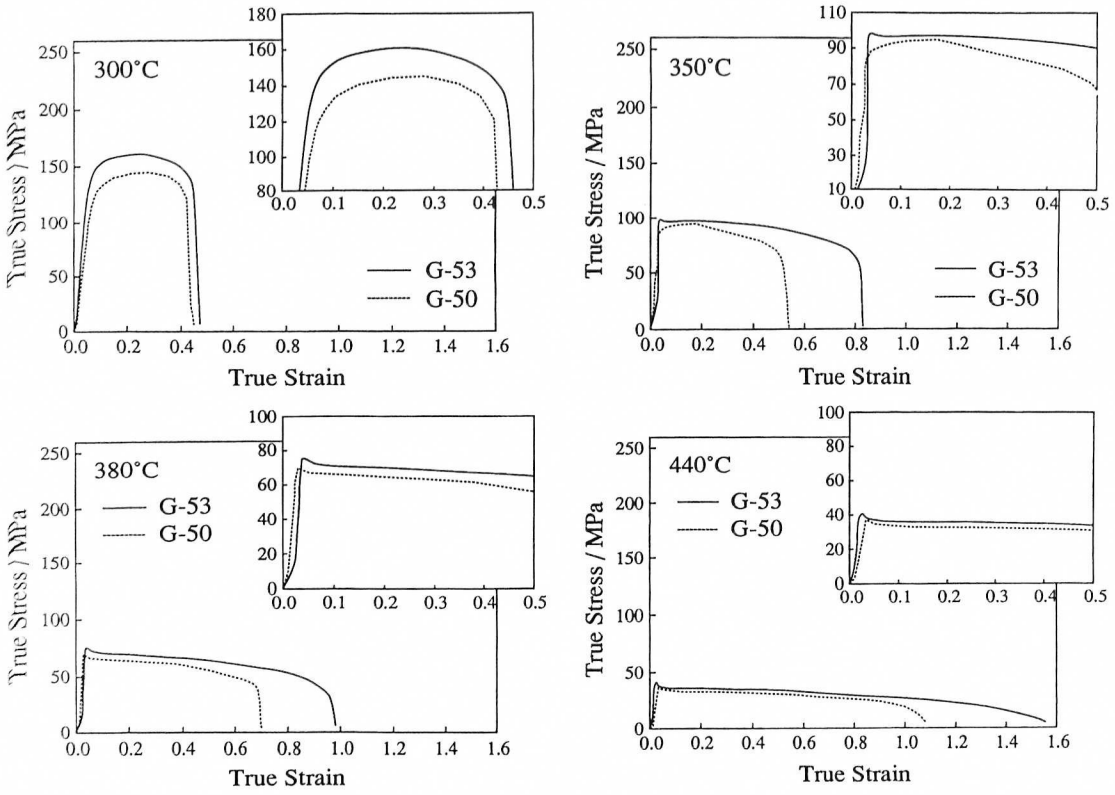

Fig. 6 Stress-strain curves of G50 (Al-5.5mass%Mg) and G53 (Al-5.5mass%Mg-0.3mass%Cu) alloys

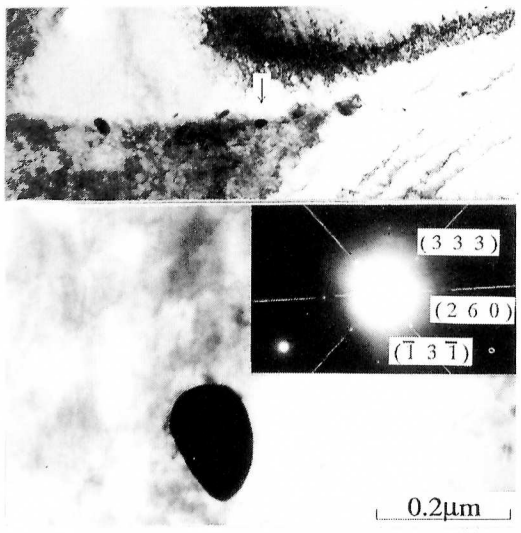

Fig. 7 TEM bright field image and diffraction pattern of T-phase in G53 (Al-5.5mass %Mg-0.3mass%Cu) alloy deformed at 380°C and a strain of 0.049

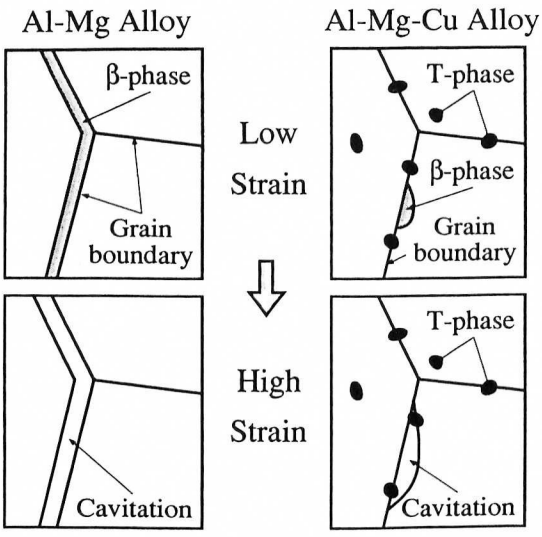

Fig. 8 Schematic comparison of cavity formation during the hot deformation